JTTEE5 10:637-642

The Deformation and Cooling of Ceramic Particles Sprayed with a Thermal Radio-Frequency Plasma under Atmospheric Conditions

B. Dzur, H. Wilhelmi, and G. Nutsch

(Submitted 16 May 2000; in revised form 28 November 2000)

Common thermal-spray techniques use the strong acceleration of powder particles to produce dense ceramic coatings with high bond strength. The residence time of the powder particles within the plasma jet is correspondingly low, and only relatively small particles can be molten. In this work, on the contrary, an inductively coupled radio-frequency (RF) inductively coupled plasma (ICP) torch was used to spray large oxide-ceramic powder particles under atmospheric conditions. The slow plasma flow of a RF plasma leads to large residence times of the powder particles, so that the powder size of the feedstock can be 100 μm and more. It was observed that these particles will not be strongly accelerated in the plasma and that their velocity at the moment of impact is in the range of 10 to 20 m/s. Ceramic coatings were ICP sprayed with a low porosity and a high bond strength, similar to direct current (DC) or high-velocity-oxygen-fuel (HVOF) sprayed coatings. The morphology of ICP-sprayed particles on smooth steel surfaces, as a function of the surface temperature, is described and compared with DC plasma-sprayed splats. Furthermore, the degree of deformation was measured and determined by different models, and the pronounced contact zones formed between the pancake and the substrate were investigated. The ICP-sprayed ceramic coatings show some special properties, such as the absence of metastable crystalline phases, which are common in other spray technologies.

Keywords alumina coatings, coating formation, microstructure, particle deformation, plasma spraying, RF inductively coupled plasma

1. Introduction

Recently, the development of various thermal-spraying technologies has led to continuously increasing particle velocities. The aim is to increase the kinetic energy of the particles in order to minimize the coating porosity and to maximize the bond strength. As is shown in Table 1 (from Ref 1), the measured and computed values of particle velocities differ strongly with the spray technology used.

In contrast to the common technologies, particles will not be strongly accelerated by the laminar flow of a large-volume plasma jet, generated by an inductively coupled radio-frequency (RF) inductively coupled plasma (ICP) torch under atmospheric conditions. This method of plasma generation and its use in thermal spraying has become a growing field of interest in the last few years. Nevertheless, special low-pressure applications with high particle velocities[2,3] are the majority of the known applications of ICP spraying. Using an ICP torch under atmospheric conditions for plasma spraying (IC APS) of materials, such as alumina and zirconia, the spraying of large powder particles with a low impact velocity also leads to the same high-coating quality.

B. Dzur, H. Wilhelmi, and **G. Nutsch,** Technische Universität Ilmenau, FG Plasma und Oberflächentechnik, Kirchhoffstraße 1, D-98684 Ilmenau, Germany. Contact e-mail: gabriele.nutsch@tu-ilemnau.de.

2. Experimental Setup

The principle of the generation of ICP and the torch used have been described previously.[4] The torch was run with argon as the plasma gas with 6.7 slpm, sheath gas with 33.3 slpm, and carrier gas with 2 slpm. The plate power was 12 kW; the frequency was 3.7 MHz.

Alumina (99.5% Al_2O_3) and yttria-stabilized zirconia (YSZ) powder (8 wt.% yttria) with a particle size between 80 and 100 μm are sprayed onto smooth, mild steel substrates at a spraying distance of 170 mm, measured from the powder injection point, with various substrate temperatures for the examination of the particle deformation, and on sandblasted, mild steel substrates for producing coatings, both under atmospheric conditions.

Furthermore, single particles and coatings of alumina are sprayed, using a DC APS system made by MEDICOAT AG (Maegenwil, Switzerland), using an argon/hydrogen gas mixture (88 vol.%, 12 vol.%) with the total gas flow rate of 50 slpm and a current intensity of 600 A. The powder size used is 5 to 45 μm.

3. Results and Discussion

3.1 Plasma and Particle Properties

Some important plasma properties, such as plasma temperature and composition, were measured with an enthalpy probe system made by TEKNA Plasma Systems, Inc. (Sherbrooke, Canada). The measured isotherms are shown in Fig. 1.

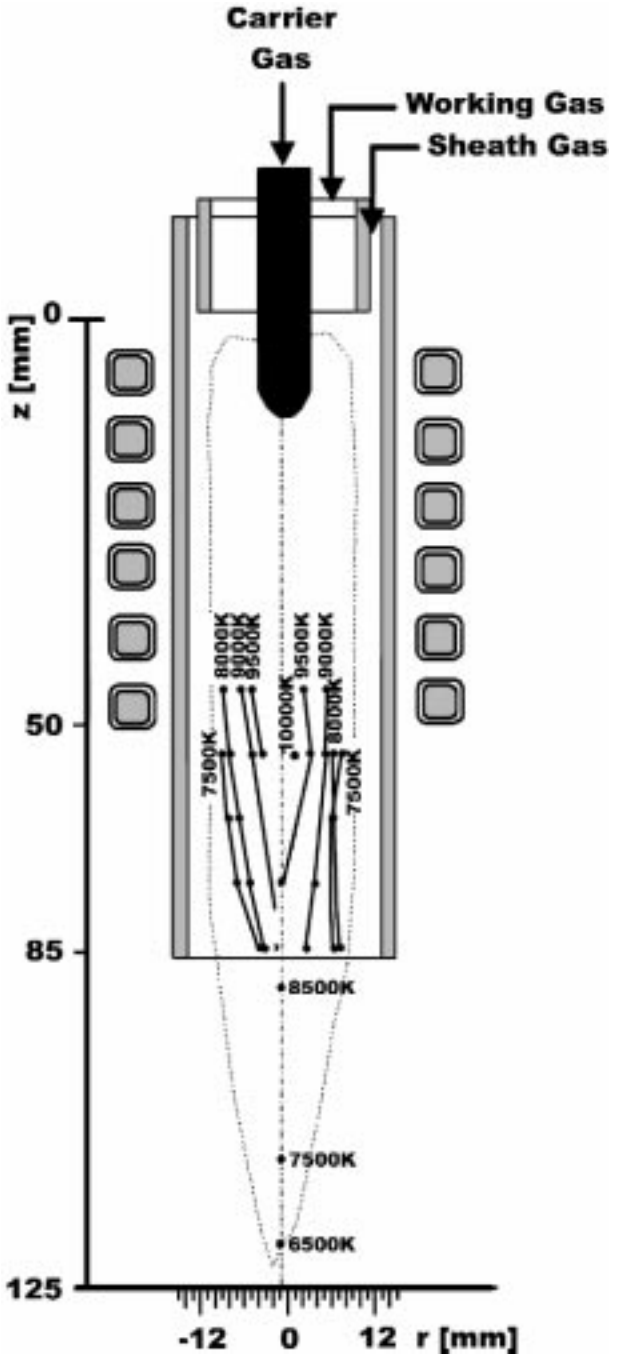

Fig. 1 Temperatures measured by enthalpy probe inside and outside the ICP torch used

The plasma velocity reaches values of about 80 m/s at the end of the torch. The laminar plasma flow results in relatively small comingling with the ambient air, as shown in Fig. 2. Only 4 vol.% oxygen is detected at an axial distance of 110 mm from the plasma tip because of the low plasma velocity and the shielding effect created by the sheath gas cover.

The particle velocity was measured by evaluating the temperature-time plots obtained with the high time-resolution pyrometer system, which is described in more detail in Ref 5. The mean particle velocity at the moment of impact was found to be

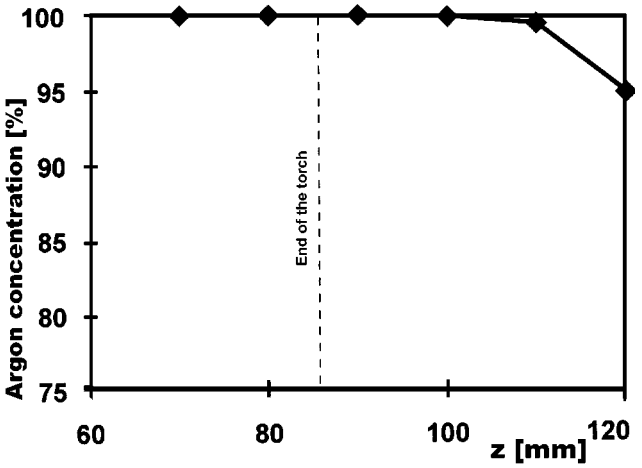

Fig. 2 Argon concentration along the plasma axis

Table 1 Mean values of the particle velocity[1]

Technology	Particle velocities (m/s)
Flame and arc spraying	50–100
Atmospheric DC-plasma spraying	150–300
Low pressure (vacuum) DC-plasma spraying	400–500
High-power plasma spraying	500–700
HVOF spraying	400–700
Detonation gun	700–800

10 m/s. This value is nearly the same order as the inlet velocity of the cold gas-carrier flow. So, the particles are little accelerated by the plasma flow.

3.2 Particle Deformation on Smooth Steel Surfaces

The typical splat morphology of ICP-sprayed alumina and zirconia particles, as a function of the substrate temperature, is shown in Fig. 3. The direct current plasma (DCP) sprayed alumina splats are shown for comparison purposes.

On nonoxidized substrates, the so-called pancake structure (circular disks with no significant ragged edges) is obtained with IC APS at substrate temperatures above 350 °C. However, the so-called flower structure is generally predominant only for DCP-sprayed particles.

According to the literature, particles will form the pancake structure at dimensionless Weber numbers, We, smaller than 80,[6,7] which can be confirmed by our results shown in Table 2.

The degree of deformation can be defined as

$$\xi_1 = \frac{\overline{D}_{\text{Pancake}}}{\overline{d}_{\text{Particle}}} \qquad \text{(Eq 1)}$$

where $\overline{D}_{\text{Pancake}}$ is the mean diameter of the splat taken from more than five splats, and $\overline{d}_{\text{Particle}}$ is the mean diameter of the powders.

This value, ξ_1, increases from 1.4 at the substrate temperature of 100 °C to 2.7 at the substrate temperature of 400 °C for alumina and for YSZ from 1.2 at 100 °C substrate temperature to 2.3 at 400 °C. The lower degree of deformation for YSZ can be explained by the lower thermal conductivity of this material.

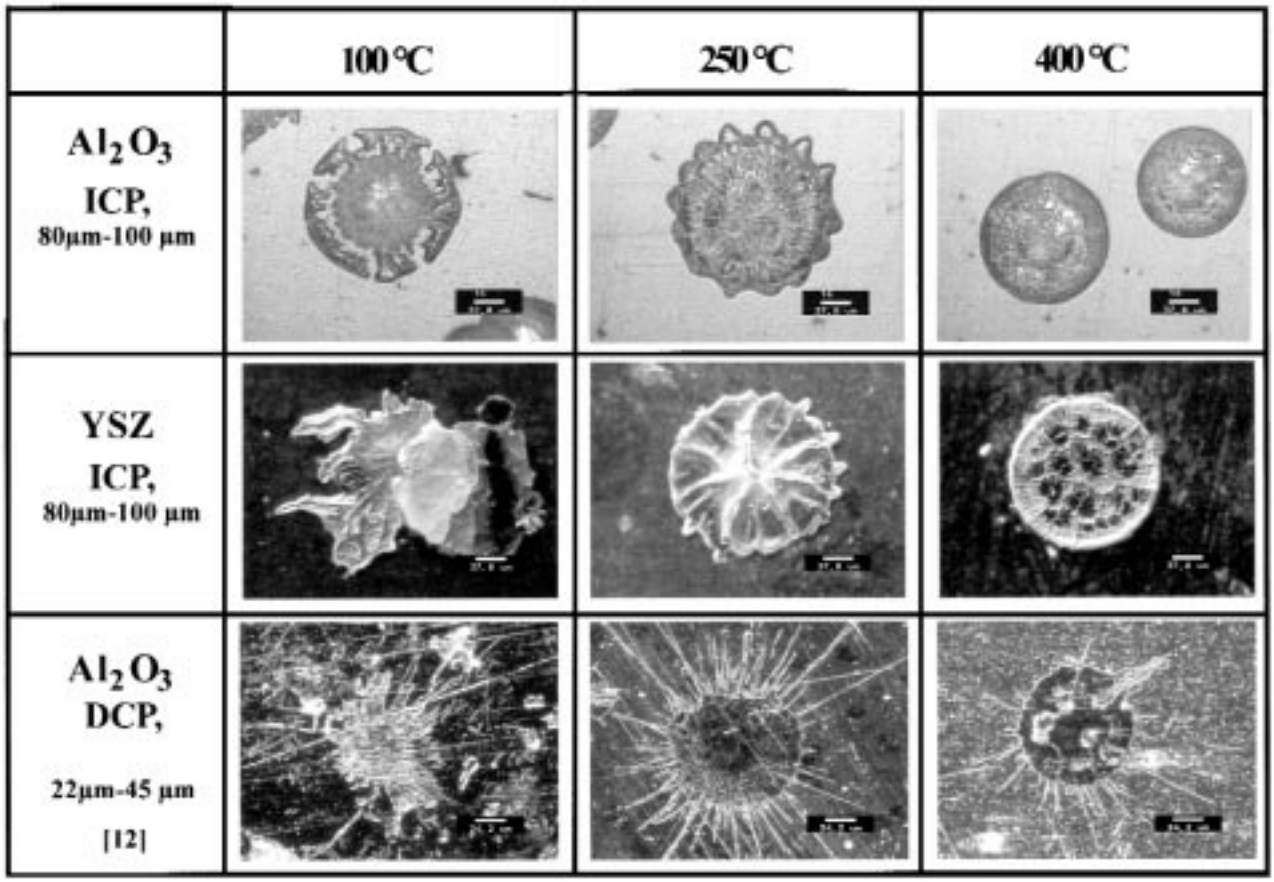

Fig. 3 Typical splat morphology depending on the substrate temperature for alumina and YSZ sprayed with IC APS and DC APS (the bar in the ICP splats is 37.8 μm, and the bar in DC splats is 24.7 μm)

Table 2 Reynolds and Weber numbers for alumina particles

Plasma conditions	Re	We
ICP (80 μm, 10 m/s)	71.2	41.3
DCP (30 μm, 200 m/s)	292.5	3391.3

This leads to a nonhomogenous temperature distribution within the particle. Thus, the temperature in the center of a particle will be lower with a corresponding higher viscosity than in the peripheral regions of the particle.

Comparing the results for alumina with various models given in the literature, a good agreement was found with the model, suggested by Wachters and Westerling:[11]

$$\xi = 0.631\mathrm{We}^{0.39} \quad \text{(Eq 2)}$$

Calculations by other models[8,9,10] using the dependency on the Reynolds number for the calculation of the degree of deformation lead to lower values than the observed ones.

The time of cooling down to the substrate temperature of such large alumina particles is of the order of 150 μs measured by the high time-resolution pyrometer.[5] Therefore, the cooling rate is about 10^5 K/s. This value is more than one order of magnitude lower than for measured values of the DCP-spraying processes.

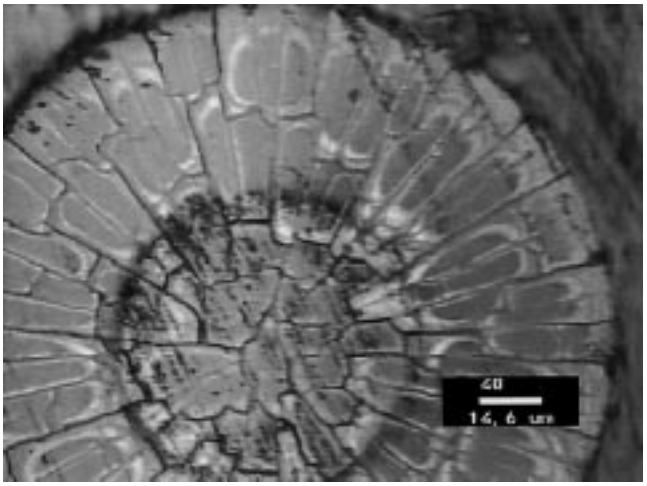

Fig. 4 Microcracks in the YSZ pancake (the bar is 14.6 μm)

A higher magnification of a YSZ pancake (Fig. 4) shows a distinct network of microcracks as a consequence of the cooling down of the particles. Microcracks can also be seen in alumina pancakes, and such microcracks are also found on DC-sprayed

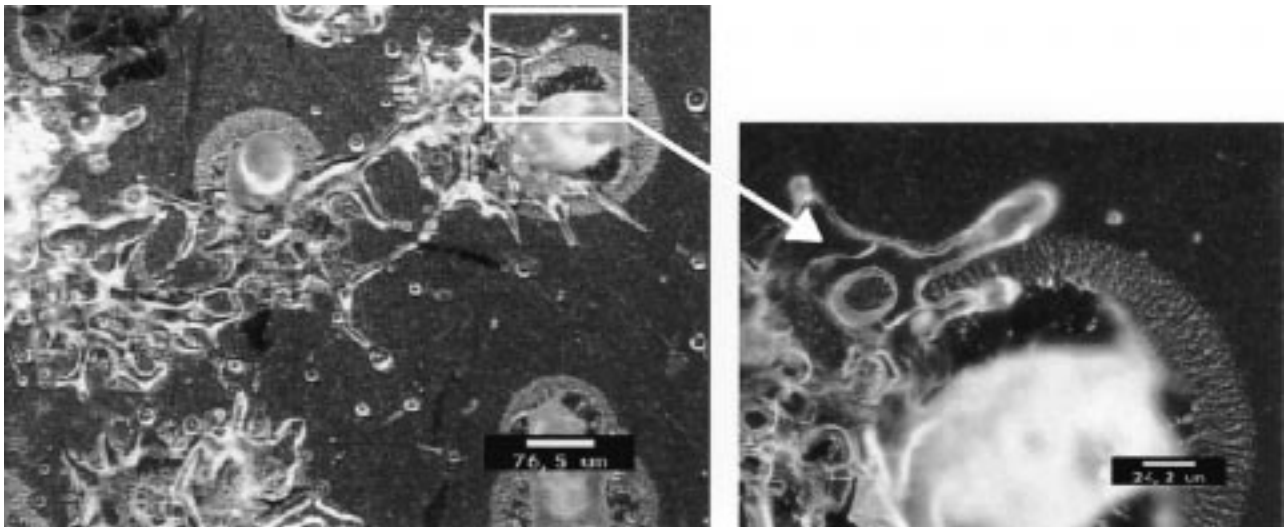

Fig. 5 Deformation of an alumina particle on a hot and oxidized steel surface (the bar on the left is 76.5 μm, and the bar on the right is 24.2 μm)

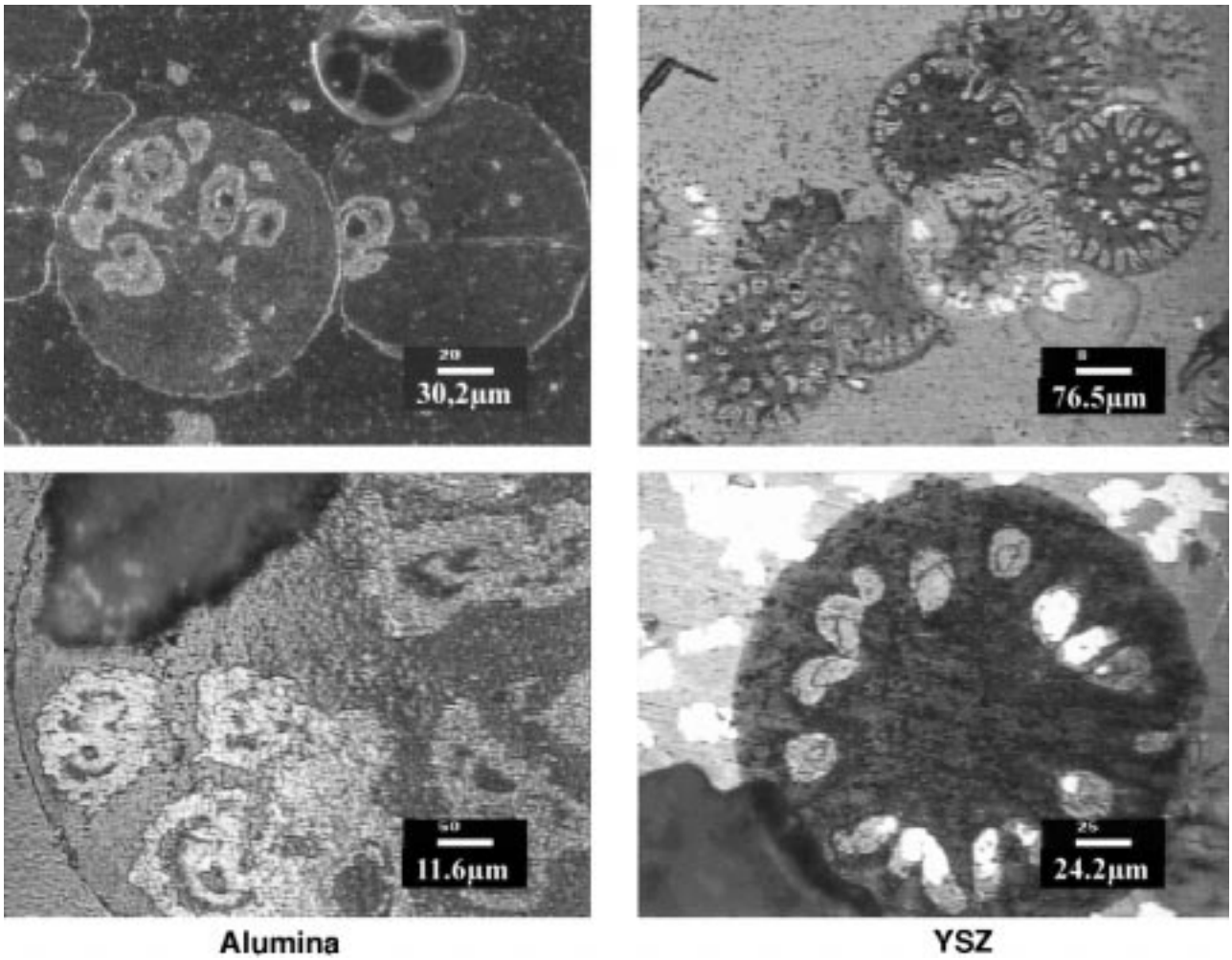

Fig. 6 Typical contact zones of impacted alumina and ziconia particles

splats. In some cases, gas bubbles are enclosed within the pancakes. This suggests that some of the particles are still boiling at the moment of impact, and/or the bubbles are formed by desorption of adsorbed gases during their flight through the plasma.

Moreover, the result shows that pancakes cannot be formed at high substrate temperatures and strongly oxidized substrates.

The deformation obtained is similar to the low substrate-temperature deformation. In this case, the liquid material cannot move on the oxide layer to form a pancake (Fig. 5). Because of this impeded deformation, some liquid material is flung away and forms a corona around the rest of the particle.

3.3 The Formation of Contact Zones

It is well known that the particles are definitely bonded onto the substrate surface in contact zones. Here, the cooling of the particles by heat conduction will take place, and some diffusion processes may occur. A high degree of contact zones is, therefore, an important condition for a high bond strength. Figure 6 shows such contact zones for alumina and YSZ.

Portions of 75 to 80% of the splats are in close contact with the substrate for the two materials. However, a regular arrangement of such contact zones is found only for YSZ (Fig. 6). Possibly, this is caused by another deformation phenomenon dependent on the formation of a bulge at the edge and a depression at the middle of the pancakes due to the different viscosities in the two regions.

Furthermore, for alumina, it was observed that most of the pancakes have melted the steel surface. The temperature near the melting point and higher of the incoming alumina particle yields contact temperatures higher than the melting point of the 400 °C preheated steel substrate.[13] This leads to an additional anchoring of the particles and following from that to higher bond strength. This effect is expected for YSZ-particles where no melting is observed. Contact temperatures, T_C, of ceramic particles on steel at 400 °C calculated after the model given in Ref 12 are listed in Table 3 for various particle temperatures, T_p. As it is shown, the T_C can reach the melting point of steel (≈1700 K) only for alumina not for YSZ.

3.4 Particle Deformation during Coating Buildup

The superposition of the pancakes in the process of coating formation leads to a distinct lamellae structure. Figure 7 shows typical lamellae in a cross section of an alumina coating. The procedure for manufacturing the metallographic cross cuttings and polishing is quite different from preparing other spray coatings due to the big and hard lamellae. It is described more in detail in Ref 14. From the well-prepared metallographic pictures, the deformation degree can be estimated by measurement of lamella thickness and length (diameter). The thickness of the accentuated lamella is 19 μm, and a mean value of 15 μm taken from 10 measurements is obtained. This value is 5 to 10 times higher than for DC-sprayed samples.[16]

With the measured length representing the diameter of lamellae, a mean value of the deformation degree of 2.5 can be derived. This suggests that the deformation mechanism caused by superposition of lamellae is the same as can be observed with impinging splats onto a smooth steel surface. However, because of the more unfavorable conditions of heat transfer to the subjacent lamella, the contact temperatures between the lamellae are higher than between splat and steel substrate.

By using the model for computing the solidification time, taken from Ref 12, and assuming the impinging particle rises to its melting temperature, values of 34 μs for alumina and 400 μs for zirconia are found. These solidification times decrease with increasing particle temperature.

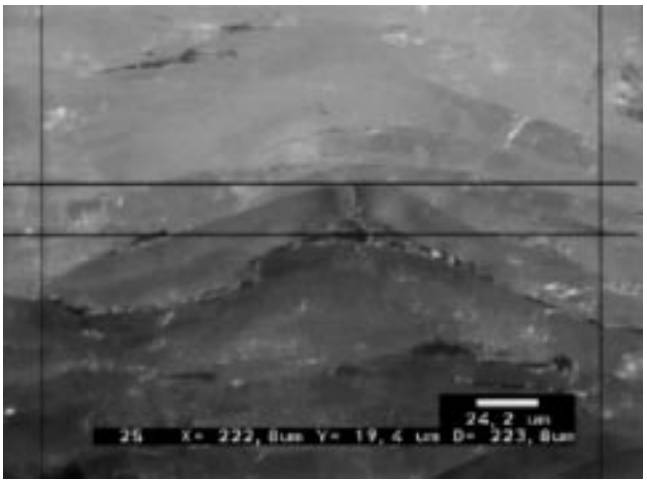

Fig. 7 Metallographic picture of an ICP APS-sprayed alumina coating (the bar is 24.2 μm, the lamella thickness is 19.4 μm, and its length is 222.8 μm)

Table 3 Contact temperatures, T_c, for ceramic particles on steel substrates

	T_C (K)	
T_P	Al_2O_3	YSZ
Melting point	1621	1031
Melting point + 500 K	1832	1099
Boiling point	1996	1337

3.5 Coating Properties

Ceramic coatings are ICP sprayed with a very high powder efficiency, which reached values of more than 90% for Al_2O_3 on tubes as well as flat samples. This is caused by nearly 100% melting of the powder in the plasma (measured during powder treatment experiments, Ref 5).

Table 4 lists some measured properties of ICP- and DCP-sprayed coatings. It is seen that under IC APS conditions, where there is only a low kinetic energy of the impinging particles, dense coatings can be sprayed. The higher porosity of the YSZ coatings arises because the impinging droplets are partially hollow. The measured bond strength of the DCP-sprayed alumina samples is slightly higher than the ICP-sprayed one. It seems that the mechanic anchoring between flower-structured splats could be stronger than between pancake-shaped splats. On the other hand, a measured bond strength of 60 MPa for ICP is in the range of typical values given in the literature for DCP coatings (*e.g.*, Ref 16). Thus, a high particle velocity is not the only way to produce high quality coatings.

The most interesting property of an ICP-sprayed coating is the minimum amount of metastable crystalline phases. Metastable phases, such as γ alumina, are predominant in DCP coatings.[16] A phase transformation always occurs during the solidification process when metal ions, which have a lower diffusion velocity than the oxygen ions, have no time to reach their

Table 4 Properties of as-sprayed ceramic coatings

Kind of powder and plasma	Porosity (%)	Bond strength (MPa)
Al_2O_3, ICP	<5%	up to 60
Al_2O_3, DCP	<4%	up to 75
YSZ, ICP	<8%	up to 60

final and stable position within the oxygen ion lattice.[15] This takes place at such high cooling rates, which are typical for DCP or HVOF. Therefore, IC atmospheric-plasma spraying of ceramics without phase transformations is possible because of the low cooling velocity of large and thick lamellae. This could open a wide field of applications of ICP-sprayed ceramic coatings in the future.

4. Summary and Conclusions

Large and slowly moving ceramic particles, typical for ICP spraying under atmospheric conditions, are leading to a special feature of deformation and cooling down after their impact onto a substrate surface. They form pancakes instead of flower structures, and the cooling rate is also one order of magnitude lower than in DC spraying.

Although the kinetic energy of ICP-sprayed particles is low in contrast to DCP, coatings of nearly the same quality can be produced. The examination of the deformation is a useful tool for explaining the typical buildup of ICP-sprayed coatings and some of their special properties. The mechanism of particle deformation is the same for the superposition of single splats within the coating as on smooth steel surfaces. The most important feature of ICP-sprayed ceramic coatings is the dominance of the thermodynamically stable crystalline phases of the sprayed material. Therefore, the ICP spray process under atmospheric conditions can complement the common technologies in the future and can even be a specialty for thermal spraying of such materials as oxide ceramics.

Acknowledgments

Part of the study was supported by the DFG and by a NSF-DAAD project. The support of the High Temperature Lab, University of Minnesota, in microstructure analysis is gratefully acknowledged.

References

1. E. Schwarz, E. Mettmann, E. Hühne, D. Grasme, and R. Kröschl: *Proc. Thermal Spraying Conf.*, TS '93, Aachen, Germany 1993, DVS Report DVS-Verlag, Düsseldorf, 1993, vol. 152, pp. 47-52 (in German).
2. R. Henne, V. Borck. M. Müller, R. Ruckdaeschel, and G. Schiller: *United Thermal Spray Conf.*, UTSC '99, Duesseldorf, 1999, E. Lugscheider and P.A. Kammer, eds., DVS-ASM, DVS-Verlag, Düsseldorf, 1999, pp. 598-602.
3. K. Fleischer, B. Wielage, M. Müller, R. Henne, and V. Borck: *United Thermal Spray Conf.*, UTSC '99, Duesseldorf, 1999, E. Lugscheider and P.A. Kammer, eds., DVS-ASM, DVS-Verlag, Düsseldorf, 1999, pp. 608-13.
4. B. Dzur and G. Nutsch: *43rd Int. Scientific Coll.*, Technical University of Ilmenau, Ilmenau, Sept. 21–24, 1998, Rektor Tu Ilmenau, Ilmenau, 1998, vol. 2, pp. 642-47 (in German).
5. B. Dzur and G. Nutsch: *12th Int. Conf. on Gas Discharges and Their Applications*, Greifswald, Germany, 1997, G. Babducke, ed., vol. 1, pp. 342-47.
6. R. Mc Pherson: *J. Mater. Sci.*, 1980, vol. 15, pp. 3141-49.
7. R. Mc Pherson: *Thin Solid Films*, 1981, vol. 83, pp. 297-310.
8. G. Trabaga and J. Szekely: *Metall. Trans. B*, 1991, vol. 22B, pp. 901-13.
9. J. Madejski: *Int. J. Heat Mass Transfer*, 1976, vol. 19, pp. 1009-13.
10. T. Yoshida, T. Oskada, H. Hamatani, and H. Kumaoka: *Plasma Sources Sci. Technol.*, 1992, vol. 1, pp. 195-201.
11. L. Wachters and N. Westerling: *Chem. Eng. Sci.*, 1966, vol. 21, pp. 1047-56.
12. J.M. Houben: Ph.D. Thesis, Technical University of Eindhoven, Eindhoven, Netherlands, 1988.
13. B. Dzur: Ph.D. Thesis, Technical University of Ilmenau, Ilmenau, Germany, 2001 (in German).
14. S. Zakharian: *Proc. 7th Workshop Plasmatechnology*, June 24–25, 1999, G. Nutsch, ed., Technical University of Ilmenau, FG Plasma and Surface Engineering, Ilmenau, 1999, pp. 73-78 (in German).
15. G. Erwin: *Acta Cryst.*, 1952, vol. 5, p. 103.
16. H.C. Chen, E. Pfender, B. Dzur, and G. Nutsch: *J. Thermal Spray Technol.*, 2000, vol. 9, pp. 264-73.